J Fluoresc (2008) 18:519–526
DOI 10.1007/s10895-007-0294-x

ORIGINAL PAPER

A Fluorescence Analysis of ANS Bound to Bovine Serum Albumin: Binding Properties Revisited by Using Energy Transfer

Denisio M. Togashi · Alan G. Ryder

Received: 22 October 2007 / Accepted: 19 November 2007 / Published online: 21 December 2007

Abstract Determination of binding parameters such as the number of ligands and the respective binding constants require a considerable number of experiments to be performed. These involve accurate determination of either free and/or bound ligand concentration irrespective of the measurement technique applied. Then, an appropriate theoretical model is used to fit the experimental data, and to extract the binding parameters. In this work, the interaction between bovine serum albumin (BSA) and 1-anilino-8-naphthalene sulphonate (ANS) is revisited. Using steady state fluorescence spectroscopy, the binding isotherm of BSA/ANS was obtained applying the Halfman–Nishida approach. The binding parameters, site number, and binding site association constants, were determined from the stoichiometric Adair model and Job's plot. The binding parameters obtained were then correlated to the distance of the respective binding site to the tryptophan residues using the energy transfer technique. This approach, that uses both tryptophans independently from each other, is presented as a tool to help understand the binding mechanism of the albumin fluorescent complex. The results show that ANS molecules bind to BSA in up to five different binding sites. Energy transfer from the tryptophan residues to the BSA/ANS complex shows that the four highest affinity binding sites ($>10^4$ M^{-1}) are located at a reasonably close distance (18–27 Å) to at least one of two tryptophan residues, while the lowest affinity binding site ($\sim 10^4$ M^{-1}) is located over 34 Å away from the both tryptophans.

Keywords Bovine serum albumin · 1-anilino-8-naphthalene sulfonate · Ligand binding · Energy transfer

D. M. Togashi (✉) · A. G. Ryder
Nanoscale Biophotonics Laboratory, Department of Chemistry,
National University of Ireland, Galway,
Galway, Ireland
e-mail: denisio.togashi@nuigalway.ie

D. M. Togashi · A. G. Ryder
National Centre for Biomedical Engineering Science,
National University of Ireland, Galway,
Galway, Ireland

Introduction

Serum albumin, in humans, accounts for about 60% of the total serum content. It is the most abundant of the plasma proteins. The main features that distinguish the primary structure of serum albumin from other extracellular proteins are the presence of only one cysteine group (Cys-34), and low tryptophan content. The secondary structure of serum albumin consists of approximately 67% of α-helix. There are nine loops and 17 disulphide bridges, which make a heart-shaped 3D structure revealed by X-ray crystallography studies [1]. The 3D structure is commonly represented by three homologous domains (I, II, and III) which are divided into two sub-domains (A and B) [2]. Human and Bovine Serum Albumins (HSA and BSA, respectively) are probably the most studied serum albumin proteins. Although, they are approximately 76% homologous, the main difference between the two proteins is that in HSA there is only one tryptophan amino acid (Trp-214), whereas in BSA there are two tryptophan units (Trp-134 and Trp-212) [2]. The principal function of serum albumin is to transport a wide variety of fatty acids, hormones, metal ions, and metabolites. The binding characteristics in serum albumin are derived from molecular forces such as hydrogen bonding, electrostatic, and hydrophobic interactions present in the different binding sites [2, 3].

Determination of the number of binding sites and their properties such as affinity and specificity towards particular ligands is accomplished by obtaining the equilibrium constants between ligands and protein. This is undertaken with the aid of different and independent techniques such as spectroscopy, calorimetry, and potentiometry [4–6]. In general, the Fluorometric titration approach is the most widely used because of its intrinsic sensitivity and simplicity. However, the determination of binding constants and binding site number depend on, in some cases, experimental conditions that are disregarded in assumptions and approximations in the model used for data analysis. Experimental artefacts such as low fluorescence intensity due to the inner filter effect often lead to erroneous results [7, 8], and must therefore be taken into account.

The binding constants and binding site numbers for 1-anilino-8-naphthalene sulfonate (ANS) with Bovine serum albumin (BSA) vary considerably between reported studies: some values, at a pH~7.0, range from 2×10^5 to 6.2×10^6 M^{-1}, and $n=1$ to $n=10$ binding sites per protein molecule [6, 9–15]. In order to understand and clarify this problem, the interaction between bovine serum albumin and 1-anilino-8-naphthalene sulfonate is revisited using the Adair's and Job's plot methods. Also, the binding parameters were correlated geometrically with tryptophan residues by using the energy transfer model described in this work.

Experimental

Materials Bovine serum albumin (BSA) of purity 99+ % (catalogue no. A7638) and 1-Anilino-8-naphthalenesulfonic acid hemi-magnesium salt hydrate (ANS) of purity 90+% were purchased from Sigma and Fluka, respectively. All reagents were used without further purification. Phosphate buffered saline tablets for 0.01 M phosphate buffer (PBS), 0.0027 M potassium chloride, and 0.137 M sodium chloride at pH 7.4 were purchased from Aldrich. All solutions were made up with purified water from a Milli-Q Millipore system.

Samples preparation In the experiments we used fresh stock protein solution in PBS at pH=7.4, which were kept in the dark at a temperature of 4 °C. The BSA concentration for stock solution was calculated using molar extinction coefficient ε_{280}=43600 M^{-1} cm^{-1} [10]. Protein final concentrations varied from 1×10^{-6} to 1.4×10^{-5} M.

Apparatus Absorption spectra were recorded with a Shimadzu UV-1601 UV-visible spectro-photometer and steady state fluorescence emission and excitation measurements on a Cary Eclipse spectrofluorimeter, in 1 cm pathlength Quartz cells. All measurements were made at room temperature.

Methods The fluorescence titrations were carried out by a constant addition of ANS solution to a BSA solution, and the final concentrations were corrected by taking into account the final volume. The fluorescence intensities were corrected to account for the inner filter effect by using Eq. 1 [7, 8]:

$$F_{\mathrm{corr}} = F_{\mathrm{meas}} \frac{2.303 \times D_{380} \times (d_2 - d_1)}{10^{-D_{380}\times d_1} - 10^{-D_{380}\times d_2}} \quad (1)$$

The fluorescence intensity is corrected by multiplying the measured intensity, F_{meas}, which is obtained measuring the absorbance and fluorescence of the ANS solutions at 380 nm. D_{380} is the absorption per centimetre at 380 nm. The parameters d_1 and d_2 are the distances, in centimetres, along the front face of the excitation [7, 8]. The distances d_1 and d_2 are determined by measuring the fluorescence intensity of ANS in water at 530 nm and the absorption at 380 nm, for a range of ANS concentrations from around 10^{-6} to 10^{-4} M, in a 1 cm pathlength cuvette. A linear relationship between the fluorescence intensity versus absorption is recovered by using Eq 1.

A Job's plot analysis [16] was used to determine the binding stoichiometry of the BSA-ANS fluorescence complex. In this approach, the molar fractions of ANS and BSA were varied while keeping the total concentration ([ANS]+[BSA]) constant. The fluorescence intensity was measured and plotted versus the ANS molar fraction. Linear regression fittings were made at the two extremes of the curve. The cross point between the two linear plots provided the amount of ANS (molar fraction) for the binding stoichiometry of the fluorescent complex. In the energy transfer experiments, the protein concentration was 1.5×10^{-6} M and the excitation wavelength was set at 280 nm. The fluorescence intensity of protein was corrected by taking into account the fraction of the excitation light absorbed by the added ANS. All the non linear fittings were performed in Excel®. The 3D model structure was built using Swiss-PdbViewer software [17].

Results and discussion

The determination of binding parameters of a specific ligand to protein, using fluorometric titration methods, involves the addition of a non-fluorescent (or very low fluorescent) ligand solution in the non-fluorescent (or very low fluorescent) protein solution which produces a fluorescent binding complex. The fluorescence intensity of this bound complex is measured and, the magnitude depends on reagent concentration. When the binding sites of the protein under investigation are totally saturated by ligand mole-

cules, the fluorescence emission intensity becomes constant. No changes should be observed for any further ligand addition. However, care must be taken when the concentration of ligand or protein molecules reaches high values such that the reactant fluorescence and/or absorption of excitation light becomes relevant.

BSA/ANS binding complexes

As mentioned above, there is a large range of reported binding constants and binding sites per protein in the literature for the BSA/ANS complex [6, 9–15]. We believe that there are three main reasons for the broad range of reported binding constant values and the existence of more than one type of binding site: (a) overlooking the inner filter effect on experimental data, (b) the method used to estimate the free ligand concentration, and (c) the use of the Scatchard's plot method instead of the Adair stoichiometry model (Eq. 2) [18–20]. Klotz et al. have already called attention in great detail to the problems related to the use of Scatchard plot to interpret binding processes, and the need not to draw hasty conclusions [21, 22].

The binding constants and the number of binding sites per protein are determined in this work by applying the Adair equation:

$$r = \frac{\sum_{1}^{N} i \times \left(\prod_{1}^{i} K_j \right) \times [\mathrm{ANS}]^i}{1 + \sum_{1}^{N} \left(\prod_{1}^{i} K_j \right) \times [\mathrm{ANS}]^i} \tag{2}$$

Where r is the average number of bound ANS per protein, or the ratio between concentration of bound ANS, $[\mathrm{ANS}]_B$, and total concentration of BSA, $[\mathrm{BSA}]_T$. N is the total number of binding sites, each K is a stoichiometry binding constant, [ANS] is the free ligand concentration.

One critical point in ligand–acceptor binding studies is to determine the amount of free ligand in the presence of acceptor. The free ANS concentration is obtained from the difference between total ANS concentration and bound ANS concentration. The most widely used approaches for calculating the free ANS concentration is to obtain a calibration curve of the system at high concentration of protein for a low range of ANS concentrations. In this case, it is assumed that all ANS molecules are fully bound to the protein, and that the fluorescence intensity is directly proportional to the bound ANS concentration. Halfman and Nishida developed a more precise method for the determination of free ligand concentration [23]. This technique involves the determination of at least two binding isotherms for different protein concentrations (e.g., a and b). Therefore, the free ligand concentration $[\mathrm{ANS}]_{a,b}$ can be determined using the following equations:

$$r_{a,b} = \frac{[\mathrm{ANS}]_{T,a} - [\mathrm{ANS}]_{T,b}}{[\mathrm{BSA}]_{T,a} - [\mathrm{BSA}]_{T,b}} \tag{3}$$

$$[\mathrm{ANS}]_{a,b} = \frac{[\mathrm{BSA}]_{T,a} \cdot [\mathrm{BSA}]_{T,b}}{[\mathrm{BSA}]_{T,a} - [\mathrm{BSA}]_{T,b}} \left(\frac{[\mathrm{ANS}]_{T,a}}{[\mathrm{BSA}]_{T,a}} - \frac{[\mathrm{ANS}]_{T,b}}{[\mathrm{BSA}]_{T,b}} \right) \tag{4}$$

Where $[\mathrm{ANS}]_{T,a}/[\mathrm{BSA}]_{T,a}$ and $[\mathrm{ANS}]_{T,b}/[\mathrm{BSA}]_{T,b}$ are the molar ratios of the total ligand concentration and total protein concentration, which correspond to the same value of average number of bound ANS per protein in the binding isotherms a and b ($r_{a,b}$). Although, the quantity r is not measured directly, it is, in general, proportional to the ratio of fluorescence intensity F and protein concentration. In other words, the concentration of bound ligand is proportional to the fluorescence intensity F. Figure 1a shows the experimental binding isotherms for five different protein concentrations. The $F/[\mathrm{BSA}]_T$ values at high ligand concentration are very sensitive to the protein small concentration variations. Therefore, the initial protein concentration values were corrected assuming that the all isotherm reaches approximately the same $F/[\mathrm{BSA}]_T$ at infinite ligand concentration. The total ligand concentrations values for the five isotherms that have the same $F/[\mathrm{BSA}]_T$ values (Fig. 1b), were estimated by cubic interpolations of the corresponding experimental data in Fig. 1a. The final binding isotherm is represented by the plot of r versus free ligand concentration (Fig. 1c). This result is generated from the average values of r and [ANS] obtained from Eqs. 3 and 4, from all the possible paired combinations of five total isotherms found in Fig. 1b (a–b, c–d, a–e,...). Finally, the binding parameters of BSA/ANS complex can be determined applying the Adair equation (Eq. 2) to the isotherm in Fig. 1c. The binding constants that represent the best fit curve of the isotherm point in Fig. 1c are shown in Table 1.

The Job plot (also known as the method of continuous variation) shown in Fig. 2 is a very useful method for the characterization of products formed by an interaction of two species. The Job method has been applied to cases where more than one type of complex is formed in the system under study [24]. The curvature observed at the top of the curve in Fig. 2 may be due to more than one type of complex. Analysis of the Job plot in Fig. 2 shows that at 380 nm excitation wavelength, the intercept between the best two straight lines occurs at a molar fraction (x_{ANS}) around 0.78. This result is in agreement with a reported value [15]. The corresponding stoichiometry is 1:3.4. At the

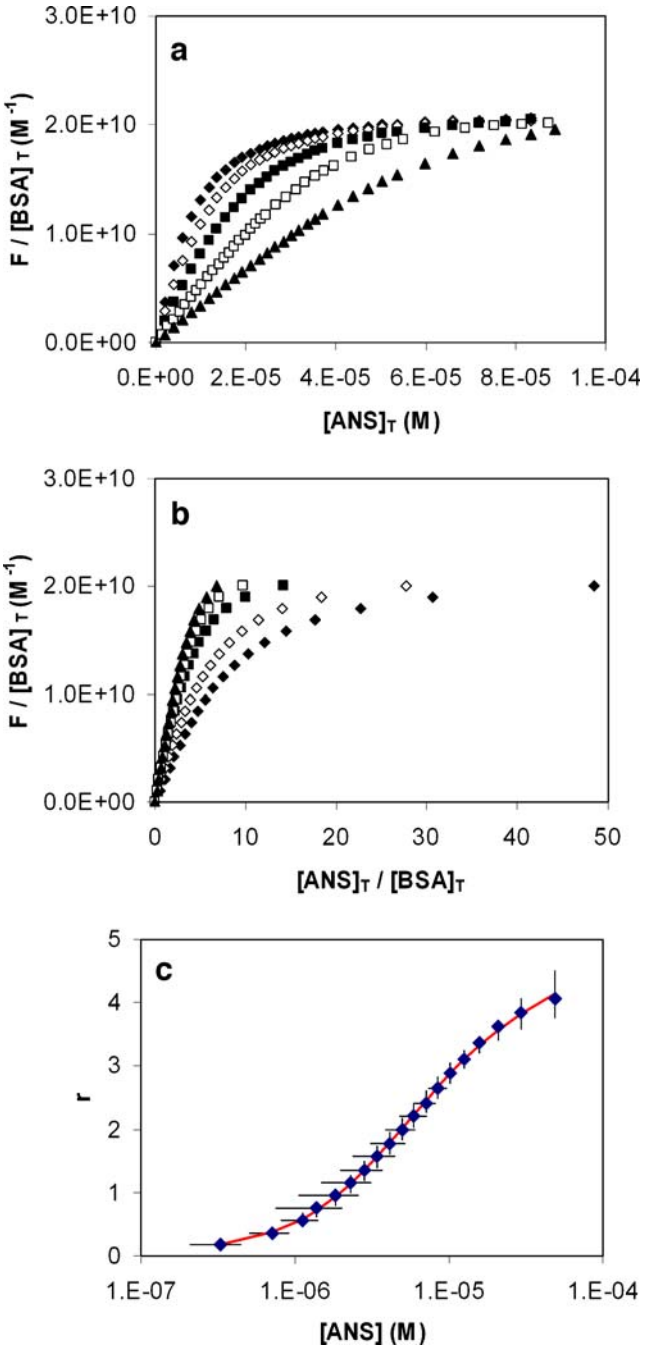

Fig. 1 BSA/ANS complex formation at different concentrations of ANS and BSA (**a**). The isotherms obtained from cubic interpolation of data points for same ordinate values (**b**) are used to build the final binding isotherm by using Halfman–Nishida approach (**c**). Protein concentrations in **a** and **b**: (*filled diamond*) 1×10^{-6} M, (*empty diamond*) 2×10^{-6} M, (*filled square*) 4.8×10^{-6} M, (empty square) 8.2 10^{-6} M, and (*filled triangle*) 1.4×10^{-5} M. The line curve in (**c**) is the best fit curve using the Adair equation. The error bars are estimated from the standard deviation between the isotherms generated after Halfman–Nishida treatment

region where the complex is formed, the crossing point is higher than the top of the experimental curve. This may indicate that the dissociation constants of the complex (inverse of binding constants) have the same order of magnitude as the total concentration used [16]. In fact, the range of values for the binding constants found from above (Table 1) corresponds to a range of 1.9×10^{-6} to 8.3×10^{-5} M for the respective dissociation constants. The total concentration used for Job plot (2×10^{-5} M) is between the above range of dissociation constants. In this case, the stoichiometry found from the plot is normally underestimated [16]. Considering the values of binding constants (Table 1) and the total concentration used for Job plot, the correct stoichiometry value is estimated to be 1:4, 1:5, or 1:6. It is important to note that non-linear curve fitting of the data points in Fig. 1c using 4 and 6 binding sites (1:4 and 1:6 stoichiometry) resulted either in bad quality of fit curves or high binding constant error values.

Table 1 Binding site parameters for the interaction of BSA/ANS complex

Binding site	Binding constants (10^4 M^{-1})	Distance from Trp-134 (R_0)	Distance from Trp-212 (R_0)
1	52±3	1.47	1.04
2	30±5	1.11	1.09
3	13±5	1.25	0.83
4	7.8±3.4	0.76	1.30
5	1.2±0.7	1.70	1.42

The results obtained here by analysis using the Adair equation (Eq. 2) on the fluorimetric titration and Job plot indicates that there are 5 binding sites. Although the nature of the binding interaction of ANS with the protein bovine serum albumin is well accepted to be hydrophobic [10, 14], others non-covalent interactions such as electrostatic and hydrogen bonding may compete within hydrophobic interactions. The balance of such forces may be responsible for the different affinities observed for ANS binding sites in BSA. Matulis et al. concluded that there are at least two different modes for ANS binding to BSA [14]. In the first

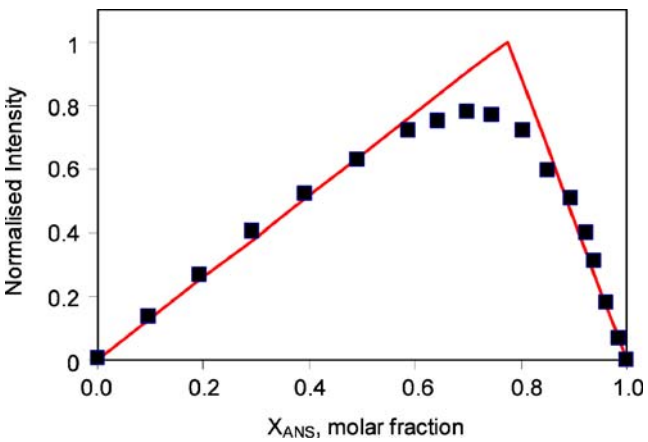

Fig. 2 Job plot for BSA–ANS fluorescence at 380 nm excitation with total concentration $[BSA]+[ANS]=2\times10^{-5}$M, and PBS buffer pH=7.4

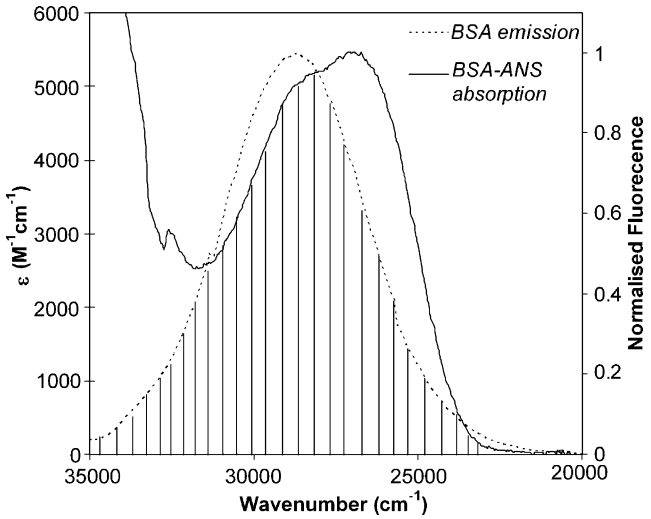

Fig. 3 Spectral overlap of BSA–ANS absorption and BSA fluorescence

mode, where five sites were found, ANS is inside the hydrophobic cavity far away from water molecules, and these ANS molecules fluoresce. These findings are in agreement with our results.

We also demonstrated that by constructing a Job's plot using fluorescence that the information on the number of binding sites is also relevant. Therefore, it is important to combine the fluorescence titration experiments (Adair analysis) with the Job's plot in order to better characterize the binding parameters, and to provide the background from which one can localize the binding sites on BSA/ANS system by energy transfer experiments. The results are well in agreement with some crystallographic data, as described below.

Energy transfer from tryptophan residues to bound ANS

Förster resonance energy transfer (FRET) in donor–acceptor pairs is a method used to determine the distance between two centres if certain conditions are followed such as: (a) good overlap between the absorption spectrum of the acceptor and the emission spectrum of the donor; (b) high fluorescence quantum yield of the donor; and (c) correct orientation of the donor and acceptor dipoles. When these conditions are met, large Förster radius values, R_0, for FRET are obtained (see Eq. 9 in the Appendix). The significant overlap between spectrum of the two tryptophans in the BSA emission and the ANS absorption spectrum is shown in Fig. 3. The value of R_0 calculated for the FRET between the two tryptophans and the bound ANS was 24 Å. This value is in good agreement with the literature values [25, 26]. Therefore, the presence of ANS molecules in BSA at a distance smaller than R_0 will cause a reduction, by FRET, of more than 50% of the tryptophan fluorescence.

In Fig. 4a, it is observed that the increase of ANS concentration causes a reduction of the BSA fluorescence band intensity at 320–380 nm and an increase of the complex fluorescence band intensity at 420–620 nm. This indicates that the energy transfer efficiency is dependent on ANS concentration. Therefore, the plot of energy transfer efficiency as a function of ANS concentration, shown in Fig. 4b, was obtained from the use of Eq. 11 (Appendix).

Since the hydrodynamic radius for BSA is ca. 35 Å [27], it is not difficult to foresee that energy transfer should occur mainly within the BSA–ANS complex. The energy transfer in a collisional complex is less efficient because the Förster radius is smaller than the hydrodynamic radius. Moreover, from the average fluorescence lifetime for BSA (around 5.6 ns [25]) and diffusion constant (59 $\mu m^2\ s^{-1}$ [28]), the diffusion limited rate constant can be estimated to be $1.6\times 10^9\ M^{-1}\ s^{-1}$. If the energy transfer only occurs due to diffusional contact, we can estimate, using the Stern–Volmer equation [29] that, the concentration of ANS in the buffer solution must be around 0.1 M to reduce the BSA fluorescence by 50%. However, as can be observed in Fig. 4b, the total concentration of ANS for a reduction of 50% of BSA fluorescence is around 10^5 times lower than the concentration expected, for the diffusional quenching case only. Therefore, FRET within the complex is the main

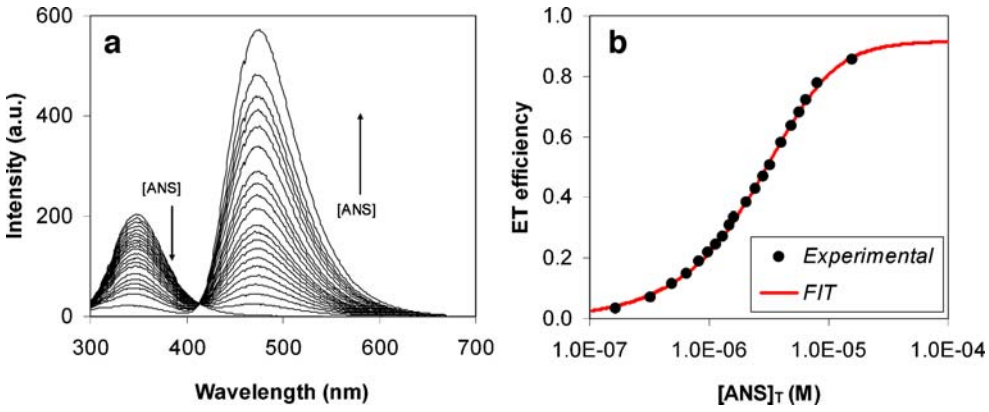

Fig. 4 **a** Fluorescence spectra of BSA with increasing ANS concentration with 280 nm excitation. **b** Energy transfer efficiency as a function of the ANS concentration. *Closed symbols* represent experimental data, and line curve is the fitted model (see text)

process responsible for the reduction in tryptophan residues emission and increase of emission from bound ANS, when the protein is excited.

The relative high FRET efficiency implies that ANS binds to a site within the protein that is close enough to interact with the emitting Trp residues. Considering that ANS binds to BSA in five sites (from the results above) a range of energy transfer efficiencies is expected.

In the present study, we use an approach, which takes into account the energy transfer efficiency between tryptophan residues and ANS bound at different binding sites. As a first approximation, we assume that there is no energy transfer between the tryptophan residues since the Forster radius (6–12 Å) [30] is very small by comparison to the distance between them in the serum albumin (~36 Å). Each one of the binding sites presented in the protein is located at a distance R_a and R_b, in Förster radius units, from Trp-134 and Trp-214, respectively. The energy transfer rate constant between tryptophan residues and n bound ligands, is defined by:

$$k_{ET}(n) = \tau_D^{-1} \cdot \sum_{\omega=1}^{n} \left(\frac{1}{R_{a,\omega}^6} + \frac{1}{R_{b,\omega}^6} \right) \tag{5}$$

τ_D is the fluorescence lifetime of donor in the absence of acceptor. However, Eq. 5 is only valid if all of the n binding sites are occupied. In practice, the amount of occupied binding sites will depend on the concentration of ligand present. In other words, it will depend on the binding affinities of the acceptor, or the probability of finding n ligand bound to the protein. This probability can be described in terms of the probability function $\Omega(n)$, which can be directly related to the fraction of concentration of bound protein with different degree of occupation in the total of N binding sites to the total bound protein concentration:

$$\Omega(n) = \frac{\left(\prod_1^n K_i \right) \times [\mathrm{ANS}]^n}{1 + \sum_1^N \left(\prod_1^i K_j \right) \times [\mathrm{ANS}]^i} \tag{6}$$

Therefore, the ET rate constant of n occupied sites for a ligand concentration [ANS] is redefined as:

$$k_{ET}(n) = \tau_D^{-1} \cdot \Omega(n) \cdot \sum_{\omega=1}^{n} \left(\frac{1}{R_{a,\omega}^6} + \frac{1}{R_{b,\omega}^6} \right) \tag{7}$$

In the overall calculated energy transfer efficiency, the total contribution of each of the n occupied sites must be taken into account. Thus, the total ET efficiency from the tryptophans to the bound ligands, within a ligand concentration [ANS], can be described as:

$$E = \frac{\sum_1^N k_{ET}(n)}{\tau_D^{-1} + \sum_1^N k_{ET}(n)} \tag{8}$$

The ET efficiency (E) is then related to the degree of occupied binding sites through the use of Eqs. 7 and 8, and together with the binding parameters determined previously, it allows the distance between the respective binding sites to Trp-212 and, to Trp-134 in BSA protein to be estimated.

Using the binding parameters from Table 1, the distance of each donor centre to the different acceptor centres can be determined independently by the non-linear fit analysis of the experimental data (Fig. 4b) obtained from fluorometric titration shown in Fig. 4a. As observed with the curve fit in Fig. 4b, the adjustment of donor–acceptor distances using the binding parameters obtained from the Adair equation shows a very good fit.

These distances calculated by this method are in agreement with values found in crystallographic studies of human serum albumin complex [31]. Our approximation of the BSA structure in Fig. 5 was based on the crystal structure of HSA complexed with arachidonic acid obtained from the Protein Data Bank (ID: 1gnj) [31]. Since BSA is very similar to HSA, we assumed that the location of Trp-134 in BSA is the same as that of the Leu-135 position in HSA. It is important to note that the number of binding

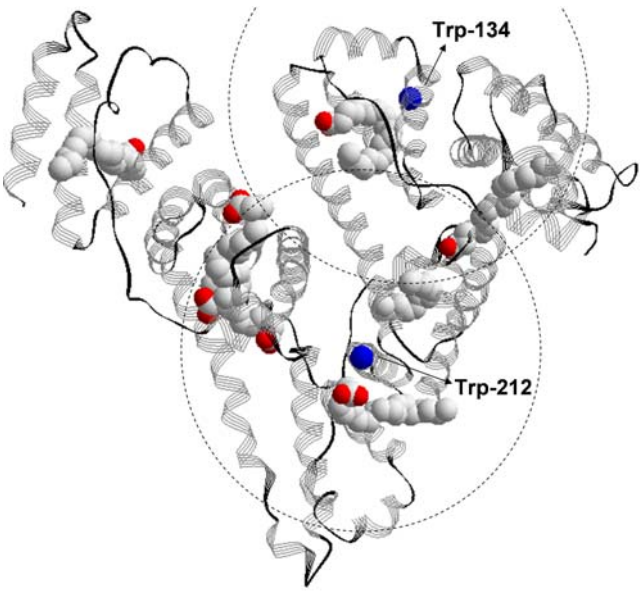

Fig. 5 Three-dimensional representation of "BSA-like" based on HSA complexed with arachidonic acid obtained from the Protein Data Bank (PDB ID: 1gnj) [31]. *Dashed circles* centred at tryptophan residues limit the region for energy transfer efficiency greater than 50%

sites in this "BSA-like" structure is based on the complex between HSA and arachidonic acid, in which there are up to seven arachidonic acids bound. However, the locations of the binding sites are approximately similar to those found for other HSA complexes [32].

Trp-212 in BSA is thought to be located in a similar hydrophobic micro-environment as the single Trp-214 in HSA (sub-domain IIA), whereas Trp-134 is considered to be more exposed to solvent and is localized in sub-domain IA [2]. In Fig. 5, the circles show the limited region for energy transfer of at least 50% of efficiency. It is interesting to note that the active region where the Trp-212 can be used as a donor centre for energy transfer involves almost all of subdomain-II, while the Trp-134 covers subdomain-I. It is at sub-domain IIA that the majority of the bound ligands are located, as observed by the arachidonic acid localisation on the "BSA-like" structure model in Fig. 5. These results agree with our findings that majority of binding sites (sites 1, 2 and 3 in Table 1) are within the Forster radius limit close to Trp-214. Also, there is only one binding site (site 4) at a distance less than the Forster radius near to Trp-134 and distant from Trp-214 (Table 1). In Fig. 5, there is also one binding site located very close to Trp-134. The "BSA-like" structure model in Fig. 5 also shows that binding sites are partially (for subdomain IIIA) or totally (for subdomain IIIB) outside the critical radius for either Trp-212 or Trp-134. Therefore, it may be expected that ANS molecules located at these sites will perform less effectively as energy transfer acceptors. In fact, the results obtained above show that binding site 5 is located far away from the regions covered by the Foster radius. We also determined from the results that this binding site is assigned to the lowest associative binding constant (K_5). This may be due to weak hydrophobic interactions between the ligand and the protein, and therefore the ligand is weakly bound. It is possible that this site is relatively more hydrophilic than hydrophobic when compared to the other binding sites. The presence of two different classes of binding sites has been reported [33] and latterly confirmed by time-resolved fluorescence studies of BSA denaturation. One class is located not too deeply in the protein interior and the other is more external and water accessible [34].

Conclusion

Using the Adair model, the Halfman–Nishida approach, and Job's plot we show that ANS binds to bovine serum albumin at five distinct binding sites. Energy Transfer from tryptophan to bound ANS shows that the binding sites are primary located close to the Trp-212 residue. The results also showed that the lowest affinity binding site (~10^4 M^{-1}) is located at an approximate minimum distance of 34 Å from the tryptophan residues (less efficient energy transfer). The sites with highest binding affinities (>10^4 M^{-1}) are found, at least for one of two tryptophan residues, close to the Forster radius distance (24 Å). This approach, combining FRET and Adair–Halfman–Nishida–Job treatments provides a more detailed method for elucidating the number and affinity of multiple binding sites in proteins. The result from this approach, correlate well with protein structural information from other sources such as crystallography.

Acknowledgement This work was supported by Science Foundation Ireland under Grant number (02/IN.1M231)

Appendix

The critical radius, R_0, in Förster resonance energy transfer is defined as the distance at which the efficiency of energy transfer is equal to 50%. It can be calculated using the following expression [29]

$$R_0 = 9780 \times \left(\kappa^2 \phi_D^0 n^{-4} J(\lambda)\right)^{1/6} \quad (9)$$

with R_0 in Å, κ^2 is the orientation factor (two-thirds assumed) describing the relative orientation in space of the transition dipoles of the donor (Trp residues) and acceptor (ANS), and ϕ_D^0 is the donor fluorescence quantum yield in the absence of the acceptor. In the case of tryptophans in BSA this value is 0.15 [35]. A value of 1.33 is assumed for the refractive index, n, of the solution. The spectral overlap integral $J(\lambda)$ between the donor emission spectrum and the acceptor absorbance spectrum was approximated by:

$$J(\lambda) = \int F_D(\lambda)\varepsilon_A(\lambda)\lambda^4 d\lambda \Big/ \int F_D(\lambda) d\lambda \quad (10)$$

where, $F_D(\lambda)$ is the normalized fluorescence spectrum of the donor and $\varepsilon_A(\lambda)$ is the absorption molar extinction coefficient.

The distance between the donor and acceptor R_{DA} can be determined by measuring the change in donor fluorescence. The donor fluorescence intensity was measured in the absence (I_D) and in the presence of acceptor (I_{DA}). Then, FRET efficiency can be calculated using the following expressions:

$$E = 1 - \frac{I_{DA}}{I_D} \quad (11)$$

References

1. He XM, Carter DC (1992) Atomic-structure and chemistry of human serum-albumin. Nature 358:209–215
2. Peters T (1985) Serum albumin. Adv Protein Chem 37:161–245

3. Kragh-Hansen U, Chuang VTG, Otagiri M (2002) Practical aspects of the ligand-binding and enzymatic properties of human serum albumin. Bio Pharm Bull 25:695–704
4. Harding SE, Chowdhry BZ (2001) Protein-ligand interactions: structure and spectroscopy. Oxford University Press, New York
5. Pacifici GM, Viani A (1992) Methods of determining plasma and tissue binding of drugs—pharmacokinetic consequences. Clin Pharmacokinet 23:449–468
6. Georgiou ME, Georgiou CA, Koupparis MA (1999) Automated flow injection gradient technique for binding studies of micro-molecules to proteins using potentiometric sensors: application to bovine serum albumin with anilinonaphthalenesulfonate probe and drugs. Anal Chem 71:2541–2550
7. Birdsall B, King RW, Wheeler MR, Lewis CA, Goode SR, Dunlap RB, Roberts GCK (1983) Correction for light-absorption in fluorescence studies of protein-ligand interactions. Anal Biochem 132:353–361
8. Eftink MR (1997) Fluorescence methods for studying equilibrium macromolecule-ligand interactions. Meth Enz 278:221–257
9. Weber G, Young LB (1964) Fragmentation of bovine serum albumin by pepsin.1. Origin of acid expansion of albumin molecule. J Biol Chem 239:1415–1423
10. Cardamone M, Puri NK (1992) Spectrofluorometric assessment of the surface hydrophobicity of proteins. Biochem J 282:589–593
11. Haskard CA, Li-Chan ECY (1998) Hydrophobicity of bovine serum albumin and ovalbumin determined using uncharged (PRODAN) and anionic (ANS(-)) fluorescent probes. J Agric Food Chem 46:2671–2677
12. Hazra P, Chakrabarty D, Chakraborty A, Sarkar N (2004) Probing protein-surfactant interaction by steady state and time-resolved fluorescence spectroscopy. Biochem Biophys Res Commun 314:543–549
13. Bagatolli LA, Kivatinitz SC, Fidelio GD (1996) Interaction of small ligands with human serum albumin IIIA subdomain. How to determine the affinity constant using an easy steady state fluorescent method. J Pharm Sci 85:1131–1132
14. Matulis D, Lovrien R (1998) 1-anilino-8-naphthalene sulfonate anion-protein binding depends primarily on ion pair formation. Biophys J 74:422–429
15. Naik DV, Paul WL, Threatte RM, Schulman SG (1975) Fluorometric-determination of drug-protein association constants—binding of 8-anilino-1-naphthalenesulfonate by bovine serum-albumin. Anal Chem 47:267–270
16. Huang CY (1982) Determination of binding stoichiometry by the continuous variation method: the job plot. Meth Enz 87:509–525
17. GlaxoSmithkline. http://www.expasy.org/spdbv/
18. van Holde KE, Johnson WC, Ho PS (1998) Principles of physical biochemistry. Prentice Hall, Englewood Cliffs, NJ
19. Scatchard G (1949) The attractions of proteins for small molecules and ions. Ann NY Acad Sci 51:660–672
20. Fletcher JE, Spector AA, Ashbrook JD (1970) Analysis of macromolecule-ligand binding by determination of stepwise equilibrium constants. Biochem 9:4580–4587
21. Klotz IM (1974) Protein interactions with small molecules. Acc Chem Res 7:162–168
22. Klotz IM, Hunston DL (1984) Mathematical models for ligand-receptor binding. Real sites, ghost sites. J Biol Chem 259:60–62
23. Halfman CJ, Nishida T (1972) Method for measuring the binding of small molecules to proteins from binding-induced alterations of physical–chemical properties. Biochem 11:3493–3498
24. Lipskier JF, Tran-Thi TH (1993) Supramolecular assemblies of porphyrins and phthalocyanines bearing oppositely charged substituents—1st evidence of heterotrimer formation. Inorg Chem 32:722–731
25. De S, Girigoswami A, Das S (2004) Fluorescence probing of albumin–surfactant interaction. J Coll Int Sci 285:562–573
26. Brocklehurst JR, Freedman RB, Hancock DJ, Radda GK (1970) Membrane studies with polarity-dependant and excimer-forming fluorescent probes. Biochem J 116:721–731
27. Axelsson I (1978) Characterization of proteins and other macro-molecules by agarose-gel chromatography. J Chromatog 152:21–32
28. Putnam FW (1975) The plasma proteins: structure, function and genetic control, vol 1, 2nd edn. Academic, New York
29. Lakowicz JR (1999) Principles of fluorescence spectroscopy, 2nd edn. Academic, New York
30. Moens PDJ, Helms MK, Jameson DM (2004) Detection of tryptophan to tryptophan energy transfer in proteins. Protein Journal 23:79–83
31. Petitpas I, Grune T, Bhattacharya AA, Curry S (2001) Crystal structures of human serum albumin complexed with monounsaturated and polyunsaturated fatty acids. J Mol Biol 314:955–960 (PDB ID: 1gnj)
32. Ghuman J, Zunszain PA, Petitpas I, Bhattacharya AA, Otagiri M, Curry S (2005) Structural basis of the drug-binding specificity of human serum albumin. J Mol Bio 353:38–52
33. Bagatolli LA, Kivatinitz SC, Aguilar F, Soto MA, Sotomayor P, Fidelio GD (1996) Two distinguishable fluorescent modes of 1-anilino-8-naphtalenesulfonate bound to human albumin. J Fluoresc 6:33–40
34. Togashi DM, Ryder AG (2006) Time-resolved fluorescence studies on bovine serum albumin denaturation process. J Fluoresc 16:153–160
35. Teale FWJ (1960) The ultraviolet fluorescence of proteins in neutral solution. Biochem J 76:381–388